



NRC Publications Archive Archives des publications du CNRC

Structure and guest dynamics in binary clathrate hydrates of tetrahydropyran with carbon dioxide/methane

Narayanan, Thaneer Malai; Imasato, Kazuki; Takeya, Satoshi; Alavi, Saman; Ohmura, Ryo

This publication could be one of several versions: author's original, accepted manuscript or the publisher's version. / La version de cette publication peut être l'une des suivantes : la version prépublication de l'auteur, la version acceptée du manuscrit ou la version de l'éditeur.

For the publisher's version, please access the DOI link below. / Pour consulter la version de l'éditeur, utilisez le lien DOI ci-dessous.

Publisher's version / Version de l'éditeur:

<https://doi.org/10.1021/acs.jpcc.5b08220>

The Journal of Physical Chemistry C, 119, 46, pp. 25738-25746, 2015

NRC Publications Record / Notice d'Archives des publications de CNRC:

<https://nrc-publications.canada.ca/eng/view/object/?id=f94ea698-f8b6-4434-9c0c-4ef83bcc3fec>

<https://publications-cnrc.canada.ca/fra/voir/objet/?id=f94ea698-f8b6-4434-9c0c-4ef83bcc3fec>

Access and use of this website and the material on it are subject to the Terms and Conditions set forth at

<https://nrc-publications.canada.ca/eng/copyright>

READ THESE TERMS AND CONDITIONS CAREFULLY BEFORE USING THIS WEBSITE.

L'accès à ce site Web et l'utilisation de son contenu sont assujettis aux conditions présentées dans le site

<https://publications-cnrc.canada.ca/fra/droits>

LISEZ CES CONDITIONS ATTENTIVEMENT AVANT D'UTILISER CE SITE WEB.

Questions? Contact the NRC Publications Archive team at

PublicationsArchive-ArchivesPublications@nrc-cnrc.gc.ca. If you wish to email the authors directly, please see the first page of the publication for their contact information.

Vous avez des questions? Nous pouvons vous aider. Pour communiquer directement avec un auteur, consultez la première page de la revue dans laquelle son article a été publié afin de trouver ses coordonnées. Si vous n'arrivez pas à les repérer, communiquez avec nous à PublicationsArchive-ArchivesPublications@nrc-cnrc.gc.ca.



Structure and Guest Dynamics in Binary Clathrate Hydrates of Tetrahydropyran with Carbon Dioxide/Methane

Thaneer Malai Narayanan,[†] Kazuki Imasato,[†] Satoshi Takeya,[‡] Saman Alavi,^{†,§,||} and Ryo Ohmura^{*,†}

[†]Department of Mechanical Engineering, Keio University, 3-14-1 Hiyoshi, Kohoku-Ku, Yokohama, 223-8522, Japan

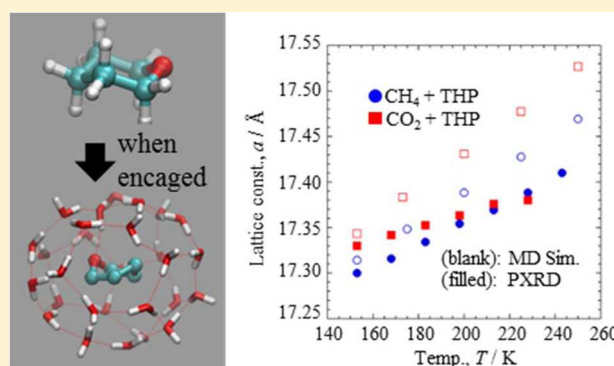
[‡]National Institute of Advanced Industrial Science and Technology (AIST), 1-1-1 Higashi, Tsukuba, 305-8565, Japan

[§]National Research Council of Canada, 100 Sussex Drive, Ottawa, Ontario K1A 0R6, Canada

^{||}Department of Chemical and Biological Engineering, University of British Columbia, Vancouver, British Columbia V6T 1Z3, Canada

Supporting Information

ABSTRACT: Binary structure II (sII) clathrate hydrates of tetrahydropyran (THP) with methane and carbon dioxide are synthesized and characterized with powder X-ray diffraction (PXRD) and molecular dynamics (MD) simulations. Analysis of PXRD results shows that 83% of the small 12-sided (dodecahedral, D) sII cages are occupied by CO₂ in CO₂ + THP hydrate, whereas 93% of the D cages are occupied by CH₄ in CH₄ + THP hydrate. The effects of the tighter fit of CO₂ molecules in the D cages of the binary hydrate were observed in longer lattice constants and lower cage occupancies compared to binary THP hydrates with CH₄ molecule in the D cage. MD simulations of 1,4-twist-boat and chair conformers of the THP in the sII clathrate hydrate phase with the CO₂ and CH₄ help gases are performed at temperatures between 153 to 250 K. Simulations suggest shape and size of D cage guest molecules does not affect the conformation of H cage guest molecule, but the steric repulsions between CO₂ molecule and cage's water molecules limits its motion and promotes interaction between H cage guest molecule and the cage at higher extent compared to CH₄ molecule.



1. INTRODUCTION

Clathrate hydrates (abbreviated as hydrates, hereafter) are a type of ice-like inclusion compounds where the guests are enclathrated by hydrogen-bonded water (host) molecules. Several clathrate hydrate structures have been identified, with the cubic structure I (sI), cubic structure II (sII), and hexagonal structure H being the most commonly occurring forms. Initially considered as a hazard in the oil and gas industry, research has come a long way to show that these materials have good potential in tackling some important environmental problems, mainly in the management of greenhouse gases. Clathrate hydrate-based gas separation technology, refrigeration systems, and gas storage methodology, in particular, for carbon capture and storage (CCS)^{1–4} are some examples of the use of clathrate hydrates in environmental applications. Despite increasing interest in clathrate hydrate based technology applications, our microscopic understanding of hydrate formation and properties is far from complete.

Hydrates with cyclic molecules as guests have held particular interest among researchers, mainly due to their large molecular size. The guest size has been suggested to affect thermodynamic stability of hydrate.^{5,6} Among cyclic molecules, studies involving cyclic ethers, ethylene oxide (EO),⁷ trimethylene oxide (TMO),⁸ tetrahydrofuran (THF),⁹ tetrahydropyran

(THP),¹⁰ as guests have been widely reported. Both EO and TMO form sI hydrates, while THF and THP form sII hydrates. Udachin et al. characterized the TMO hydrate through single crystal X-ray diffraction and reported interesting orientational order of TMO guests in the large 5¹²6² cages of the sI clathrate hydrate, which was absent for EO guests.⁸ For THF hydrates, several molecular dynamics (MD) simulation and experimental researches suggested presence of hydrogen bonding between oxygen atom of the guest ether and hydrogen atom of the host water.^{11–13} Presence of hydrogen bonding induces Bjerrum-like defects, which in turn, may contribute to guest dynamics and macroscopic properties such as hydrate formation rate and cage occupancy. Intuitively, similar interactions between THP guest and host water molecule can be expected as seen in the THF hydrate.

Udachin et al.¹⁰ synthesized crystals of THP sII clathrate hydrate in air (which lead to inclusion of nitrogen gas in the D cages) and determined the single-crystal X-ray diffraction structure of this clathrate hydrate at 100 K. They observed that the THP molecules have the boat form which occupies two

Received: August 24, 2015

Revised: October 16, 2015

Published: October 26, 2015

distinct off-centered symmetry positions in the sII hexakaidecahedral ($H, 5^{12}6^4$ or large) cages with site occupancies of 46 and 54%. The proximity of the THP guests to the cage walls maximizes possible van der Waals or hydrogen bonding contacts with the cage water molecules. In their crystal structures the distance of the THP O atom from the cage water O atoms is determined to be in the range of 3.558 to 3.704 Å, which can be consistent with hydrogen bonding.

The structure and relative energies of the gas phase conformers of THP have been studied in detail by Freeman et al.¹⁴ using quantum chemical calculations, following earlier molecular mechanics studies of Andrianov et al.¹⁵ Similar to cyclohexane, in the gas phase the most stable conformer of THP is the chair form. Tetrahydropyran has two distinct, nonenantiomeric twist-boat conformers, labeled the 1,4-twist-boat and 2,5-twist-boat, see Figure 1. In the gas phase, the 1,4-

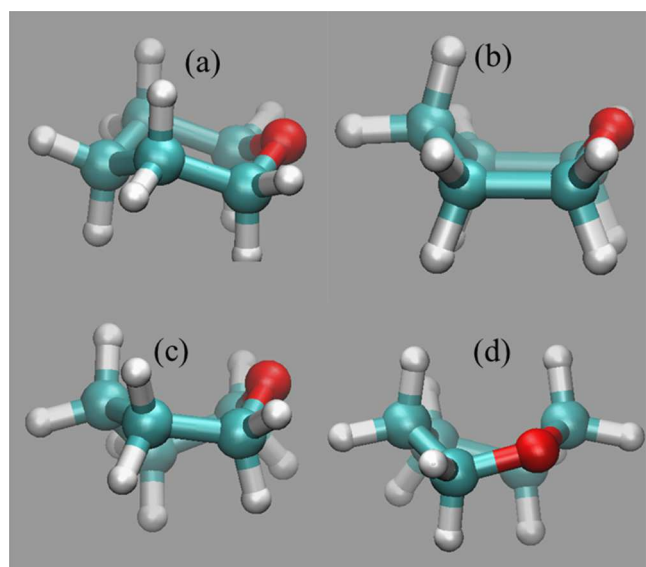


Figure 1. (a) Chair, (b) 1,4-boat transition state, (c) 1,4-twist-boat, and (d) 2,5 twist-boat conformations of tetrahydropyran. The relative energies of the conformations are given in Table 3.

twist-boat is the more stable conformer than the 2,5-twist-boat by about 1 kcal/mol. There are two boat conformers of THP, which are transition states between two twist-boat forms. The structure of the 1,4-boat conformer is shown in Figure 1.

The X-ray diffraction structure for the THP guests in the large sII cages was determined to be a boat/twist-boat conformation and not the chair form which is the most stable conformer in the gas phase.¹⁰ The boat and twist-boat conformers of THP have energies between 5.5 and 7 kcal/mol higher than the more stable chair conformation. Confinement of the THP in the clathrate hydrate cage drives the guest molecule structure from the more stable chair to the twist-boat conformation, which has a smaller effective volume.

The preference of smaller conformers of guest molecules in sII clathrate hydrate cages has been observed in the single-crystal X-ray crystallographic structure of 1-propanol hydrate¹⁶ and Raman spectroscopy and powder X-ray diffraction (PXRD) studies of *n*-butane hydrate^{17,18} as well, where gauche conformations of 1-propanol and *n*-butane were observed in the large $5^{12}6^4$ cages. A similar distortion of guest shape to favor some gauche conformations upon enclathration is also seen in a number of large guests in the sH clathrate hydrates.¹⁹ In THP,

the boat and twist-boat conformations have smaller lengths for their maximum dimensions than the chair form. See below for further discussion.

In this work, we study binary sII clathrate hydrate of THP with CO_2 and CH_4 with PXRD and MD simulation methods, as a follow up of our previous publication²⁰ with new hydrate crystal samples. The effect of CO_2 and CH_4 molecules in the small cages on the state of THP guests in the large cage and subsequently, guest–host interactions of THP in the large cage are studied. As observed in our previous study with structure H hydrate,²¹ the presence of CO_2 is expected to affect guest–host interactions of THP in the large cages to a greater extent than CH_4 , due to its long linear shape. By comparing the results obtained from simulations and experimental analysis of different hydrates, we discuss the crystal structure of $\text{CH}_4/\text{CO}_2 + \text{THP}$ hydrate more detail. We expect this study to contribute to further understanding of clathrate hydrate structure model.

2. METHODS

2.1. Powder X-ray Diffraction Measurement. Distilled water and liquid THP (of 99 mass % certified purity from Sigma-Aldrich) was used with pure CH_4 (99.99 vol % certified purity from Takachiho Chemical Industrial Co., Ltd.), pure CO_2 (99.995 vol % certified purity from Japan Fine Products Co., Ltd.) to synthesize powder CH_4 or $\text{CO}_2 + \text{THP}$ hydrate crystals, respectively.

A high pressure, stainless steel cylinder with inner volume of 200 cm^3 was used to synthesize powder $\text{CH}_4/\text{CO}_2 + \text{THP}$ hydrate crystals. The vessel was equipped with a magnetic stirrer to constantly agitate fluid and hydrate mixture. Temperature within the vessel was kept at 284 K using a PID-controlled water bath system. Pressure within the vessel was controlled by supplying or purging hydrate forming gas (CH_4 or CO_2) through a pressure-regulating valve or diaphragm valve, respectively. The temperature and pressure conditions were monitored using the platinum resistance thermometer and strain-gauge transducer connected to the inner vessel.

A 46 g of mixture of liquid THP and distilled water was added to the vessel at water-to-liquid THP molar ratio of 17:1. This ratio represents stoichiometric amount of THP needed to fill all large cages of structure II clathrate hydrate. The air in the vessel was purged by repeating pressurization of CH_4 to 1.0 MPa and depressurization to atmospheric pressure technique for three times. CH_4 (or CO_2) was then supplied to the vessel until the pressure increased to 3.0 MPa (2.7 MPa for CO_2) and line connecting the gas supply cylinder and vessel was intermittently closed. The pressure in the vessel decreased upon hydrate formation. As the pressure decreased to equilibrium condition, CH_4 (or CO_2) was supplied once again, up to 3.0 MPa (3.4 MPa for CO_2) and repeated until no further pressure reduction was observed. No pressure reduction indicates nearly complete or complete conversion of water to hydrate. All pressure conditions are set below the simple CH_4 (or CO_2) sI hydrate formation pressure range at prescribed temperature. After ensuring no further pressure reduction in the vessel, the high-pressure vessel was removed from water bath and immediately immersed in liquid nitrogen bath to prevent dissociation of hydrate samples. The vessel was disassembled, and hydrate sample remaining at the lower part of the vessel was collected and stored at temperature below 77

K. The hydrate samples were then subjected to PXRD measurements at atmospheric pressure.

PXRD measurements were performed using a laboratory X-ray diffractometer (40 kV, 40 mA; RIGAKU model Ultima-III) with parallel beam optics and a low-temperature chamber. To investigate the cage occupancies and guest positions, the PXRD data was collected over the 2θ range of $6\text{--}100^\circ$, with a step width of 0.02° . Analysis of the hydrate structures were done using Rietveld program RIETAN-FP.²² Here, the hydrate structures were initiated by a global optimization of the experimental PXRD profiles with a parallel tempering approach implemented in the direct-space technique²³ using the FOX program.^{24,25}

2.2. Computational Methods. The minimum energy structures and relative energies of the gas phase THP conformers are calculated at the MP2/aug-cc-pVDZ level of theory using the Gaussian 09 suite of programs.²⁶ The relative lengths of the THP conformers are determined from the optimized structures.

Molecular dynamics simulations on the THP hydrates are performed with DL_POLY molecular dynamics program version 2.20²⁷ on a $2 \times 2 \times 2$ replica of the sII unit cell. Coordinates of the water oxygen atoms of the clathrate hydrate phase were taken from single crystal X-ray crystallography^{7,28} and water hydrogen positions in the unit cell are determined to be consistent with the ice rules and in a manner minimizing the net unit cell dipole moment.²⁹ The centers of mass of THP, methane and CO₂ guests were initially placed at the center of the respective hydrate cages and the molecules are allowed to move freely in the cages.

In the simulations, the THP 1,4-twist-boat and chair conformations were given intramolecular flexibility and modeled with the general AMBER force field (GAFF)³⁰

$$V_{\text{tot}} = \sum_{\text{bonds}} k_b (r - r_{\text{eq}})^2 + \sum_{\text{angles}} k_\theta (\theta - \theta_{\text{eq}})^2 + \sum_{\text{dihedrals}} k_\phi [1 + \cos(n\phi - \delta)] + \sum_{i=1}^{N-1} \sum_{j>1}^N \left\{ 4\epsilon_{ij} \left[\left(\frac{\sigma_{ij}}{r_{ij}} \right)^{12} - \left(\frac{\sigma_{ij}}{r_{ij}} \right)^6 \right] + \frac{q_i q_j}{4\pi\epsilon_0 r_{ij}} \right\} \quad (1)$$

Water was modeled with the TIP4P/ice potential,³¹ CO₂ with the Harris-Yung potential,³² and CH₄ with the TRAPP potential.³³ The discussion of the contributions in eq 1 and potential parameters are given in Table S1 of the Supporting Information. A cutoff of 13 Å was used for the short-range forces in the simulation.

Constant pressure–temperature (NPT) simulations were first performed for 1.1 ns with 0.1 ns equilibration, followed by 200 ps of constant energy–volume (NVE) simulations to determine dynamic properties and hydrogen bonding. Effects of the CH₄ and CO₂ in the small cage on hydrogen bonding of the THP guests in twist-boat and chair conformations in the large cages were studied. A THP guest molecule is considered hydrogen bonded with a cage water molecule if the distance of the THF ether oxygen (OS) to a water hydrogen atom (HW) is less than 2.1 Å. Simulations are also performed for THP with empty D cages for reference.

3. RESULTS AND DISCUSSION

3.1. Structure and Guest–Host Hydrogen Bonding. PXRD Analysis. Both CH₄ + THP and CO₂ + THP crystal structures are identified to be cubic structure II. PXRD patterns

of the studied samples are presented in Figure 2. Predetermined THP conformation from MD simulations and water framework

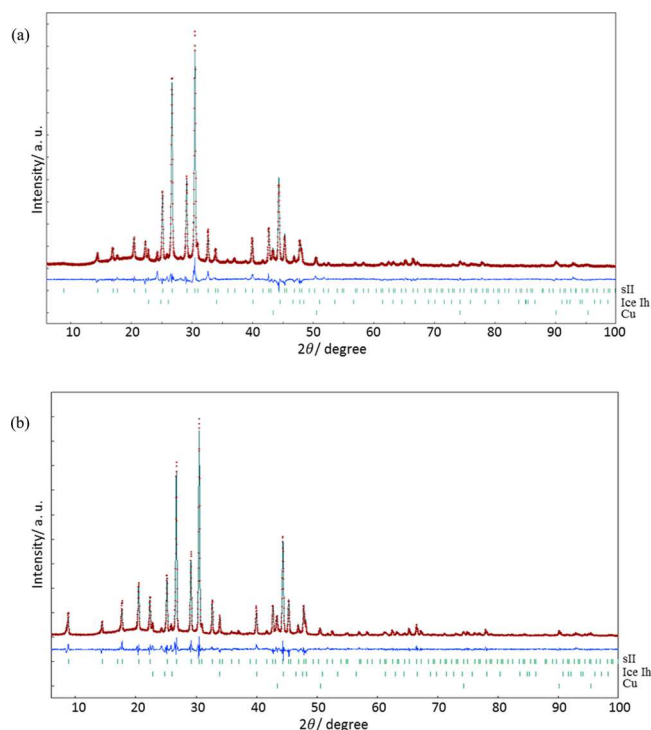


Figure 2. PXRD patterns at $T = 153$ K for (a) CO₂ + THP hydrates; (b) CH₄ + THP hydrates. Red points and black line indicate diffracted pattern and calculated pattern, respectively.

from ref 10 were used for the Rietveld refinement. Conformation of THP as 1,4-twist-boat was confirmed for both CO₂ + THP and CH₄ + THP hydrates with good agreement, R -weighted pattern (R_{wp}) of 10.1% for the former and 12.1% for the latter. Figure 3 illustrates 1,4-twist boat conformation of THP in the large H cage of CO₂ + THP hydrate. Tendency of molecules to settle in conformation with

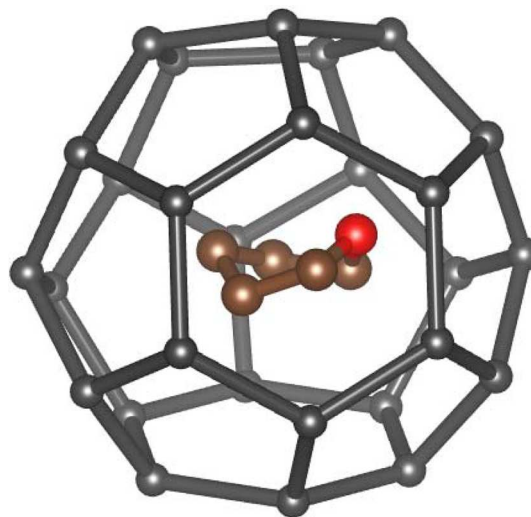


Figure 3. 1,4-Twist-boat conformation of THP in the large H cage of sII hydrate from PXRD analysis. Oxygen and carbon atoms of THP are represented in red and brown, respectively.

smaller effective radii in the hydrate cage was confirmed for both CO₂/CH₄ + THP hydrates.

The lattice constants for the sII clathrate hydrates of THP with CH₄ and CO₂ at 173 K are given in Table 1. The shortest

Table 1. Geometric Characterization of the sII THP Clathrate Hydrate Phases with Different Guests in the Small Cage from X-ray Diffraction Experiments

guest	lattice constant (Å)	small cage occupancy	$d_{\min}(\text{OS-OW})$ (Å)
THP + N ₂ ^a	17.315(7)	0.708	3.604
THP	17.3220 ^b	0.93	3.320 ^c
twist-boat + CH ₄			
THP	17.3451 ^b	0.83	3.056 ^c
twist-boat + CO ₂			

^aRef 10; 173 K. ^bPXRD this work; 173 K. ^cPXRD this work; 153 K.

heavy atom distances for the THP molecule and water framework ((CH₂)₅O...OH₂ distances) from the X-ray structural analysis of the clathrate hydrate are also given in Table 1. The experimental occupancy of CO₂ and CH₄ in the sII D cages in these clathrate hydrates was determined to be 83% and 93%, respectively. Similar structural parameters of N₂ + THP hydrate from previous literature¹⁰ are provided for reference.

The effects of nature and occupancy of the guest in small D cages are observable. PXRD measurements show that despite having greater D cage occupancy for CH₄ as compared to CO₂, the lattice constants for the CO₂ + THP phase are larger. For N₂ + THP phase, the lattice constant is similar to sII hydrate with CH₄ + THP hydrate. A larger lattice constant for the same structure suggests tighter fit of guest molecule to the cages,⁸ in this case, a tighter fit of CO₂ molecule to the 5¹² cages compared to CH₄.

Stretching of the D cage and smaller cage occupancy of CO₂ can be ascribed to asymmetrical shape of these cages in the sII hydrate³⁴ and long linear CO₂ molecule shape. Although D cage is the only common cage existing in all naturally occurring sI, sII, and sH hydrate structures, the symmetry and size of D cage is different in all three of them. The sII and sH hydrates have larger and less symmetrical small D cages than sI.^{34,35} The asymmetrical CO₂ molecules have repulsive interactions in the asymmetrical cage direction, stretching it to one direction. Longest atom to atom distance of CO₂ and CH₄ molecules are calculated to be 2.355 and 1.795 Å, respectively, determined at the b97d/6-31++g(d,p) level theory.²⁶ In comparison to CO₂, the spherical CH₄ molecule is smaller in size and fits the D cages with relative ease. Comparable length of CO₂ guest molecule to cage size³⁴ and asymmetrical shape of the D cage justifies the image that CO₂ fits into the sII 5¹² cage with difficulty and subsequently increases the lattice constant and fills only a smaller number of cages. As shown in Table 2, a similar trend can also be seen in minimum distance between the oxygen atoms of THP guests and oxygen atoms of host water molecules. Closer proximity of THP oxygen atom to the wall in CO₂ + THP hydrate may suggest expansion of the D cage in the direction toward H cage.

MD Simulations. Table 2 and Figure 4 show lattice constants of binary CO₂ + THP and CH₄ + THP hydrates and the pure THP hydrate from PXRD measurements and calculated at different temperatures using molecular dynamics simulations. The calculated lattice constants of the sII THP phases are not greatly affected by the chair or 1,4-twist-boat

Table 2. Lattice Constant, a (Å) at Different Temperatures for 1,4-Twist-Boat and Chair THP Hydrates with CO₂, CH₄ in D Cages, and Empty D Cages from PXRD Measurements and Molecular Dynamics Simulations^a

small cage guests	measured by PXRD		computed by molecular dynamics		
	T (K)	a (Å)	T (K)	a (Å)	
				1,4-twist-boat THP	chair THP
CH ₄	153	17.2998	153	17.3144	17.318
	168	17.3160	175	17.3486	
	183	17.3340	200	17.3887	17.39
	198	17.3537	225	17.4279	
	213	17.3687	250	17.4688	17.4691
	228	17.3881			
	243	17.4102			
CO ₂	153	17.3300	153	17.3465 (17.3433)	17.3423
	168	17.3413	175	17.3901 (17.3835)	
	183	17.3527	200	17.4409 (17.4305)	17.4387
	198	17.3630	225	17.4929 (17.4773)	
	213	17.3760	250	17.5439 (17.5267)	17.5406
	228	17.3800			
	empty D cages			153	17.3079
			175	17.3389	
			200	17.3748	17.3772
			225	17.4115	
			250	17.4492	17.4504

^aFor the experimentally determined 1,4-twist-boat conformation of the THP + CO₂ hydrate, lattice constants for the 100% occupied and experimentally determined 80% D cage occupied D cages (in parentheses) are given.

conformation of the THP guests in the large H cages, but nature and occupancy of the small cage guests does affect the lattice constants. For both THP molecule conformations, the lattice vector of the binary hydrate with CH₄ is predicted to be smaller than that of the binary hydrate with CO₂, which is consistent with our experimental results given in Table 1, thus, confirming the reliability of our MD results at the prescribed temperature range. The pure THP sII hydrate has the smallest lattice constant.

In the simulations, the degree of occupation of CO₂ guest molecule in the D cages contributes guest–host hydrogen bonding in the large 5¹²6⁴ H cages. The hydrogen bonding of the 1,4-twist-boat conformers of THP with water in the sII hydrates with CO₂, CH₄ gases in small cages and empty small cages is observed in the OS...HW radial distribution functions (RDF), which are shown in Figure 5. The peak in the RDF at ~1.8 Å represents the presence of THP–water hydrogen bonds. The THP–water hydrogen bond formation is endothermic and at higher temperatures the probability of formation of this hydrogen bond increases. The hydrogen bonding probability can be quantified by using the integral of the RDF graph. As seen in Figure 5, the THP–water hydrogen bonding is greatest in the binary sII hydrate of THP with CO₂. The larger size and the steric repulsion of the CO₂ guests on the sII D cages weakens the hydrogen bonds between the cage water molecules and facilitates hydrogen bonding between THP and water. Superficially, this phenomenon might be

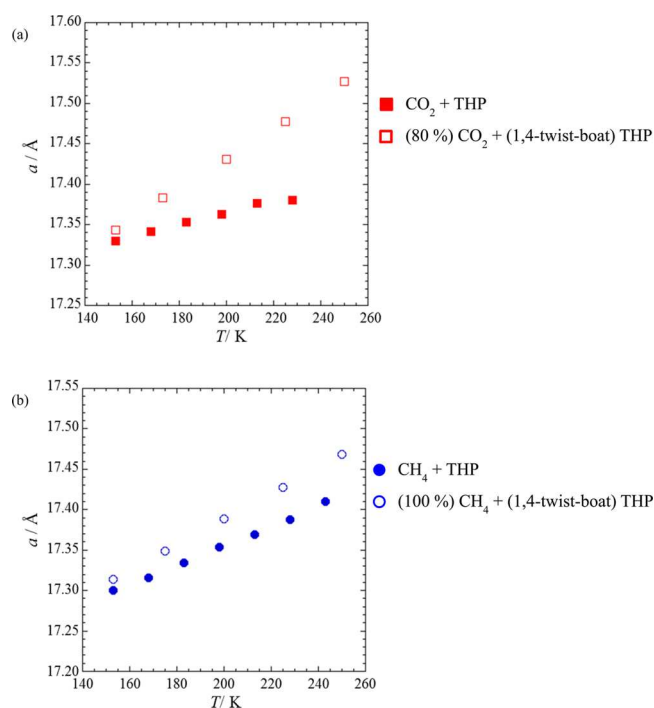


Figure 4. Lattice constants a (Å) of THP hydrates determined from PXRD measurements (filled symbol) and MD simulations (blank symbol).

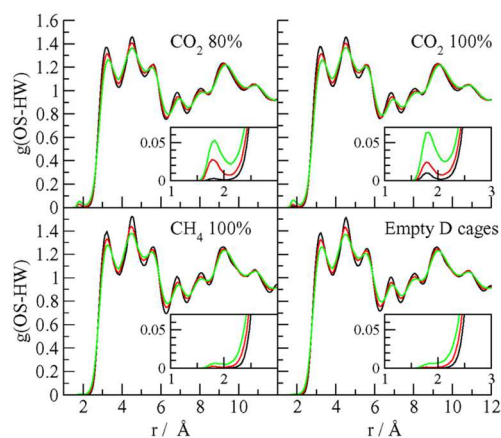


Figure 5. Radial distribution functions for the THP oxygen atom (OS) and the water hydrogen atom (HW) for the sII THP hydrates at three temperatures with 100% of D cages filled with CO_2 ; 80% of D cages filled with CO_2 (experimental composition); 100% of D cages filled with CH_4 ; empty D cages. In each case, the inset shows the peaks in the hydrogen bonding region. Green, red, and black lines represent values at $T = 153, 200,$ and 250 K, respectively.

explained by guest (CO_2)–guest (THP) interactions, but is just more likely a result of interaction between guests in both small and large cages, with a water molecule in between the cages.

Similar to our previous simulations of binary sII THF hydrates with different small cage guests,³⁶ the THP hydrates with CO_2 show the greatest degree of hydrogen bonding between the large cage guests with the lattice water. Snapshots of THP molecules in 1,4-twist-boat and chair conformations, extracted from the molecular dynamics simulations at 250 K, which show hydrogen bonding to the cage waters are shown in Figure 6. Hydrogen bonding of lattice water with THP leads to the formation of a Bjerrum L-defect between the two

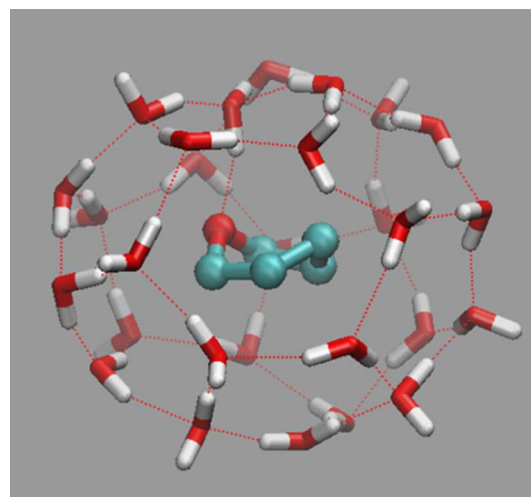


Figure 6. Snapshot of THP in the large sII clathrate hydrate cages which show hydrogen bonding with water from simulations at 250 K. Hydrogen atoms have been removed from the THP conformers for clarity.

framework water molecules which were previously hydrogen bonded. The effect of L-defects on guest dynamics is explained further below.

In previous work, we performed simulations of the sII THP hydrate with the SPC/E potential for water.¹¹ The degree of hydrogen bonding predicted with this water potential was significantly higher than the present TIP4P-ice simulation. The SPC/E potential underestimates the melting point of ice and underestimated the strength of the water–water interactions in the solid phase. This leads to a greater propensity for hydrogen bonding with other guest molecules in the hydrate phase in SPC/E simulations.³⁷

3.2. Conformation Analysis of THP in H Cage and Thermodynamic Stability. The energies of isolated THP chair, 1,4-twist-boat, and 2,5-twist-boat conformers from quantum chemical calculations are given in Table 3. The isolated THP chair conformer is more stable by 5.5–6.8 kcal·mol^{−1} than the twist-boat conformations. However, as shown in Table 3, the twist-boat conformations have smaller effective radii and are expected to be more stable in the sII H cages.

The calculated lattice constants for the clathrate hydrate phases starting with different conformers of THP and different small guests in the D cages at temperatures in the range of 150 to 250 K are given in Table 2. As mentioned above, no significant difference in lattice constant was observed between hydrates with THP in chair or twist-boat conformation.

Despite having molecular flexibility, the transformation between chair and 1,4-twist-boat conformers in the H cages was not observed within the time frame of the simulations. This can be due to the large energy barrier to gasification of these conformers (~ 11 kcal/mol in the gas phase, from quantum chemical calculations), the short time of the simulation, and the artificially high energy penalty of transformation between the conformers from the harmonic nature of the angle bending potential of the GAFF, as given in eq 1.

We compare the unit cell configurational energies (total potential energy) of the 1,4-twist boat and chair forms of THP in Table 4. At each temperature, the hydrate with the THP twist-boat conformation has a lower configurational energy than the hydrate with the chair conformation. The configura-

Table 3. Absolute Energies, Relative Energies Compared To the Chair Conformer, and Heavy Atom Distances of the THP Chair, 1,4-Twist-Boat, 2,5-Twist-Boat, and 1,4-Boat Conformers in the Gas Phase Calculated at the MP2/aug-cc-pvdz Level of Theory

configuration	energy (Hartree)	ΔE (kcal·mol ⁻¹)	$d_{\max}(\text{C}\cdots\text{O}); d_{\max}(\text{C}\cdots\text{C})$ (Å)
chair	-270.9812647		2.9077; 2.8740
1,4-twist-boat	-270.9723902	5.57	2.6655; 2.6868, 2.9698
2,5-twist-boat	-270.9708600	6.53	2.9957; 2.6984
1,4-boat	-270.9705422	6.73	2.6066; 2.8811

Table 4. Average Configurational Energy per Unit Cell, E_{config} (kcal·mol⁻¹) in 1,4-Twist-Boat and Chair THP Hydrates with CO₂, CH₄ in D Cages, and empty D Cages from Molecular Dynamics Simulations^a

THP hydrate small cage guests	temperature (K)	E_{config} (kcal·mol ⁻¹)	
		1,4-twist-boat THP	chair THP
CO ₂	153	-2169.8 (-2147.8)	-2159.6
	175	-2135.0 (-2116.3)	
	200	-2100.1 (-2080.8)	-2089.5
	225	-2069.0 (-2045.4)	
	250	-2034.0 (-2022.3)	-2004.9
CH ₄	153	-2169.4	-2158.0
	175	-2139.4	
	200	-2107.6	-2089.5
	225	-2077.0	
	250	-2046.8	-2014.9
empty D cages	153	-2069.3	-2053.6
	175	-2037.9	
	200	-2006.1	-1987.6
	225	-1975.9	
	250	-1949.8	-1914.5

^aFor the 1,4-twist-boat CO₂ hydrates, configurational energies for 100% D cage occupancy and experimental 80% D cage occupancies (in parentheses) are given.

tional energy for the hydrates 1,4-twist boat THP with CH₄ help-gas are smaller than those hydrates with CO₂ help-gas. Energies of both CH₄ + THP and CO₂ + THP phases are smaller (more negative) than the configuration energy of the sII hydrate phase with only THP in the large cages and empty small cages. This shows that the CH₄ and CO₂ guests have a net negative potential energy contribution to the hydrate phase. Unit cell configurational energy agrees with the trend in thermodynamic stability since CH₄ + THP can be formed at higher temperature, lower pressure conditions than CO₂ + THP hydrates.²⁰

Compared to the THP hydrate with empty D cages, CH₄ and CO₂ molecules both stabilize the hydrate structure. However, this stabilization effect does not correlate with hydrogen bonding formation between THP and water in the large cages. In binary hydrates with the CO₂ molecules in the small cage facilitated THP and water molecule hydrogen bonding interaction, but this enhancement does not occur in hydrates with CH₄ molecule or empty D cages. However, making generalizations that thermodynamic stability is independent of guest–host hydrogen bonding interaction, is indeed risky, as large cage hydrogen-bonding alcohols such as 2-propanol^{38–40} and 3-methyl-butanol⁴¹ are known to shift phase boundary in the pressure–temperature experimental phase diagram of CO₂ or CH₄ gas hydrate to lower temperature, higher pressure region than ether hydrates.^{20,42}

Lower thermodynamic stability of hydrates with alcohol molecules as guest in the large cage compared to hydrogen bonding ether molecules can be accounted to larger partial atomic charges on hydroxyl group atoms than ether-oxygen atom, although other factors such as size of the molecule may play an important role as well.

3.3. Guest Dynamics. The dynamics of the guests in the small cages can be studied with the normalized velocity autocorrelation function (VACF),

$$\psi(t) = \frac{\langle \sum_{i=1}^N \mathbf{v}_i(t) \cdot \mathbf{v}_i(0) \rangle}{\langle \sum_{i=1}^N \mathbf{v}_i(0) \cdot \mathbf{v}_i(0) \rangle} \quad (2)$$

where the brackets represent the ensemble average over the velocity-autocorrelation function of the central carbon atoms of the CO₂ or CH₄ guests molecules in D cages of the simulations. The VACF gives a measure of the guest rattling motions in the D cages. The VACF for the binary hydrates with CO₂ and CH₄ are given in Figure 7. The smaller and lighter CH₄ molecules move with a greater velocity range and larger rattling frequency than the larger CO₂ molecules.

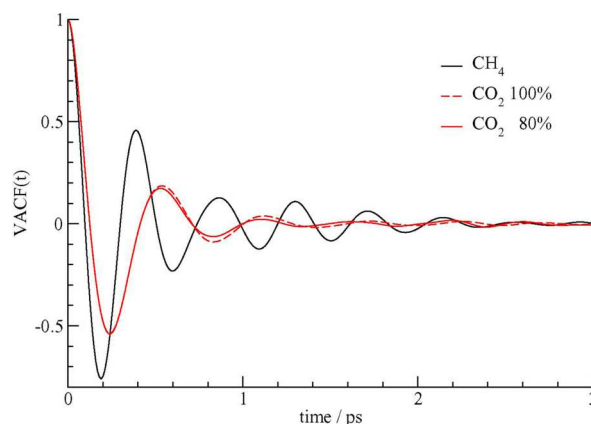


Figure 7. Normalized velocity autocorrelation functions for carbon atoms of CH₄ and CO₂ guests in the D cages of the binary sII THP hydrates at 250 K.

In addition to the vibration/rattling motion of the CO₂ guest center of mass, the rotational motion of the CO₂ guests can be studied using the orientation autocorrelation functions, $M_1(t)$ and $M_2(t)$ are defined as

$$M_1(t) = \langle \boldsymbol{\mu}(t) \cdot \boldsymbol{\mu}(0) \rangle = \langle \cos \theta(t) \rangle \quad (3)$$

and

$$M_2(t) = \langle 3 \cos^2 \theta(t) - 1 \rangle \quad (4)$$

In eq 3, $\boldsymbol{\mu}(t)$ represents a unit vector pointing along a chosen C–O bond of a guest molecule. The dot product $\boldsymbol{\mu}(t) \cdot \boldsymbol{\mu}(0)$ in eq 3 represents the cosine of the angle θ over which the

molecule has rotated between times 0 and t . The brackets represent ensemble averages over all CO₂ guests in the small cages of the simulation. The functions $M_1(t)$ and $M_2(t)$ represent the ensemble averages of the first-order and second-order Legendre polynomials for the molecule rotation, respectively. $M_1(t)$ gives an indication of the time scale for the randomization of the in-plane orientation of the molecule. The $M_2(t)$ function measures the spherical symmetry of the motion of the guest in the cage. If the motion of the guest in the cage is not spherically symmetric, the $M_2(t)$ function will not decay to zero.

The $M_1(t)$ and $M_2(t)$ functions for CO₂ in the binary THP hydrate with 100% of D cages full and with the 80% experimental D cage occupancy are given in Figure 8. The

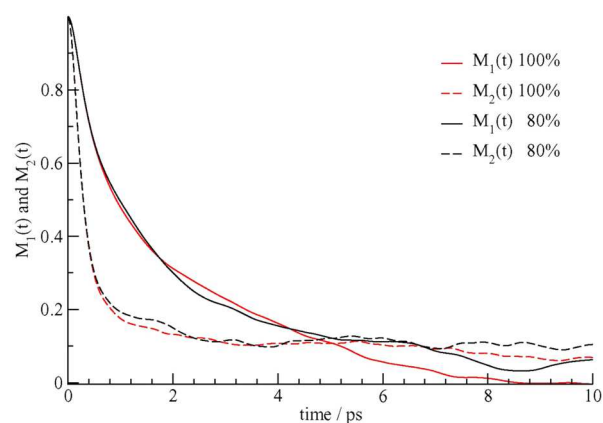


Figure 8. Rotational autocorrelation functions $M_1(t)$ (solid lines) and $M_2(t)$ (dashed lines) for CO₂ in the D cages of the binary sII hydrate with THP at 250 K. The red lines are for the hydrate with 100% CO₂ D cage occupancy and the black lines are for the hydrate with 80% D cage occupancy.

$M_1(t)$ functions decay to zero within ~ 10 ps, which is similar to behavior of CO₂ in the binary THF + CO₂ clathrate hydrates studied in ref 13. The relatively fast decay of $M_2(t)$ to a nonzero value within a time of about 2 ps is also similar in the THF + CO₂ and THP + CO₂ binary hydrates.

An interesting extrapolation may be made from the comparison of the binary CO₂ + THF and CO₂ + THP sII hydrates. In the CO₂ + THF hydrate, variations of the ¹³C NMR line shape of CO₂ showed that at temperatures above ~ 240 K, CO₂ molecules begin to migrate between adjacent small cages (from a cage occupied by CO₂ to an adjacent empty cage). Given the similarity between the hydrogen bonding to the cage water molecules between THF and THP in these two binary hydrates,¹³ it could be predicted that the CO₂ migration phenomenon observed CO₂ + THF may also be seen in the CO₂ + THP hydrate.

3.4. Volumetric Properties. Table 2 and Figure 4 show temperature dependence of lattice constants. In the range of temperature studied, almost linear expansion of lattice vector with increasing temperature was observed for all cases. Thermal expansivity between 153 and 198 K was calculated for binary THP hydrates from PXRD measurements. Thermal expansivity for CO₂ + THP and CH₄ + THP hydrates were $0.73 \times 10^{-3} \text{ \AA} \cdot \text{K}^{-1}$ and $1.20 \times 10^{-3} \text{ \AA} \cdot \text{K}^{-1}$, respectively. In the similar temperature range, between 153 and 200 K, thermal expansivity calculated using results yielded from MD simulations were $1.86 \times 10^{-3} \text{ \AA} \cdot \text{K}^{-1}$ and $1.58 \times 10^{-3} \text{ \AA} \cdot \text{K}^{-1}$ for (80% cage occupancy)

CO₂ + (1,4-twist-boat) THP and CH₄ + (1,4-twist-boat) THP hydrates, respectively. An overestimation of the expansivity by MD calculations compared to the experimental results can be observed.

Thermal expansivity is ascribed to anharmonic motion of guest molecules following increase in temperature, which weakens hydrogen bonding between water molecules consequently, expanding the cage.⁴³ Following that, tighter configuration of CO₂ guest molecule in D cages which weakens water–water interactions is expected to result in higher thermal expansivity in the CO₂ + THP hydrate compared to the CH₄ + THP hydrate, as determined from MD simulations. However, interestingly, experimentally determined results did not show a similar trend.

Several factors could be related to this anomaly. One possible factor is stronger THP and cage water molecules attraction at higher temperatures. As observed in Figure 5, MD simulations performed in this study indicate that probability of hydrogen bond formation between THP and the oxygen atom of the cage increases with temperature, which is particularly pronounced in CO₂ + THP hydrate. Attraction due to increased probability of hydrogen bonding between the molecules at different sites may inhibit expansion of the water cage, thus resulting in lower thermal expansivity for CO₂ + THP hydrates.

Another possible reason is CO₂ molecule migration between cages at high temperatures, which has been observed in CO₂ + THF hydrate, as explained above.¹³ Energy at high temperatures may contribute to translational motion of CO₂ molecule to empty cages rather than to weakening of hydrogen bond between water molecules. Besides, this anomaly may also be due to CO₂ + THP hydrate is approaching its thermodynamic stability threshold at the referred temperature range. Inability of MD simulations to capture CO₂ migration and hydrate expansion near decomposition condition may have resulted in overestimation of CO₂ + THP hydrate thermal expansivity. Further studies on thermal expansivity of structure II hydrate with CO₂ molecules in D cage are important to gain more insights on this phenomenon.

4. CONCLUSIONS

We have characterized binary sII CO₂ + THP and CH₄ + THP hydrates using PXRD analysis and MD simulations. Conformation of THP in the large H cage of sII hydrate was found to be 1,4-twist-boat, confirming preference of large cage guest molecules to obtain conformations with smaller effective volume in the hydrate cages. MD simulations gave lower configurational energies (total potential energy content) to large (H) cage twist-boat conformers of guest which are observed in the PXRD experiment. Therefore, MD may be used to choose the conformation of the guest as it is encapsulated into the hydrate cages. We have demonstrated MD configurations can help in determining initial guess for the X-ray structural determination of hydrates with cyclic molecules as guests as well as hydrocarbon molecules as guests.¹⁸

Qualitative agreement was obtained between PXRD analysis and MD simulations for predicting the effects of different help-gas species and their occupancies on the lattice constants of the binary sII THP clathrate hydrates. Shape and size of the small D cage guest molecules were found to affect the hydrate structure, but not the H cage guest conformation. Effect of tighter fit of CO₂ molecule to the D cage was observed in longer lattice constants and lower cage occupancies compared to binary THP hydrates with CH₄ molecule in the D cage. MD

simulations also suggested presence of CO₂ molecule promotes interaction between THP and the water framework to form hydrogen bonds. Analysis on guest dynamics proved that the shape and size of molecule may impose steric repulsions between the molecule and cage, thus, restricting its motion.

■ ASSOCIATED CONTENT

● Supporting Information

The Supporting Information is available free of charge on the ACS Publications website at DOI: 10.1021/acs.jpcc.5b08220.

Explanation on potential energy of the system and atomic point charges and Lennard-Jones parameters for atoms and molecules used (PDF).

■ AUTHOR INFORMATION

Corresponding Author

*Tel.: +81-45-566-1813. E-mail: rohmura@mech.keio.ac.jp.

Notes

The authors declare no competing financial interest.

■ ACKNOWLEDGMENTS

The authors would like to thank Dr. Saneshiro Muromachi (Nat. Inst. of Adv. Ind. Sc. And Tech., Japan) for his contributions during the preliminary discussions. This study was supported by a Keirin–Racing-based research promotion fund from the JKA Foundation and by JSPS KAKENHI (Grant No. 25289045).

■ REFERENCES

- (1) Tomita, S.; Akatsu, S.; Ohmura, R. Experiments and Thermodynamic Simulations for Continuous Separation of CO₂ from CH₄+CO₂ Gas Mixture Utilizing Hydrate Formation. *Appl. Energy* **2015**, *146*, 104–110.
- (2) Ogawa, T.; Ito, T.; Watanabe, K.; Tahara, K.; Hiraoka, R.; Ochiai, J.; Ohmura, R.; Mori, Y. H. Development of a Novel Hydrate-Based Refrigeration System: A Preliminary Overview. *Appl. Therm. Eng.* **2006**, *26*, 2157–2167.
- (3) Ogawa, H.; Imura, N.; Miyoshi, T.; Ohmura, R.; Mori, Y. H. Thermodynamic Simulations of Isobaric Hydrate-Forming Operations for Natural Gas Storage. *Energy Fuels* **2009**, *23*, 849–856.
- (4) Uchida, T.; Ikeda, I. Y.; Takeya, S.; Kamata, Y.; Ohmura, R.; Nagao, J.; Zatssepina, O. Y.; Buffett, B. A. Kinetics and Stability of CH₄–CO₂ Mixed Gas Hydrates during Formation and Long-Term Storage. *ChemPhysChem* **2005**, *6*, 646–654.
- (5) Takeya, S.; Hori, A.; Uchida, T.; Ohmura, R. Crystal Lattice Size and Stability of Type H Clathrate Hydrates with Various Large-Molecule Guest Substances. *J. Phys. Chem. B* **2006**, *110*, 12943–12947.
- (6) Imasato, K.; Murayama, K.; Takeya, S.; Alavi, S.; Ohmura, R. Effect of Nitrogen Atom Substitution in Cyclic Guests on Properties of Structure H Clathrate Hydrates. *Can. J. Chem.* **2015**, *93*, 906–912.
- (7) McMullan, R. K.; Jeffrey, G. A. Polyhedral Clathrate Hydrates. IX. Structure of Ethylene Oxide Hydrate. *J. Chem. Phys.* **1965**, *42*, 2725–2732.
- (8) Udachin, K. A.; Ratcliffe, C. I.; Ripmeester, J. A. Structure, Dynamics and Ordering in Structure I Ether Clathrate Hydrates from Single-Crystal X-Ray Diffraction and 2H NMR Spectroscopy. *J. Phys. Chem. B* **2007**, *111*, 11366–11372.
- (9) Sargent, D. F.; Calvert, L. D. Crystallographic Data for Some New Type II Clathrate Hydrates. *J. Phys. Chem.* **1966**, *70*, 2689–2691.
- (10) Udachin, K. A.; Ratcliffe, C. I.; Ripmeester, J. A. Single Crystal Diffraction Studies of Structure I, II and H Hydrates: Structure, Cage Occupancy and Composition. *J. Supramol. Chem.* **2002**, *2*, 405–408.
- (11) Alavi, S.; Susilo, R.; Ripmeester, J. A. Linking Microscopic Guest Properties to Macroscopic Observables in Clathrate Hydrates: Guest-Host Hydrogen Bonding. *J. Chem. Phys.* **2009**, *130*, 174501.
- (12) Conrad, H.; Lehmkuhler, F.; Sternemann, C.; Sakko, A.; Paschek, D.; Simonelli, L.; Huotari, S.; Feroughi, O.; Tolani, M.; Hämäläinen, K. Tetrahydrofuran Clathrate Hydrate Formation. *Phys. Rev. Lett.* **2009**, *103*, 218301.
- (13) Moudrakovski, I. L.; Udachin, K. A.; Alavi, S.; Ratcliffe, C. I.; Ripmeester, J. A. Facilitating Guest Transport in Clathrate Hydrates by Tuning Guest-Host Interactions. *J. Chem. Phys.* **2015**, *142*, 074705.
- (14) Freeman, F.; Kasner, M. L.; Hehre, W. J. An Ab Initio Theory and Density Functional Theory (DFT) Study of Conformers of Tetrahydro-2H-Pyran. *J. Phys. Chem. A* **2001**, *105*, 10123–10132.
- (15) Andrianov, V. M.; Zhibankov, R. G.; Krajewski, J. W.; Gluzinski, P. Isomerization Pathways in Tetrahydropyran. Mathematical Modeling of Hybrid Conformations and Vibrational Spectra of Six-Membered Heterocycles. *J. Struct. Chem.* **1990**, *31*, 399–405.
- (16) Udachin, K.; Alavi, S.; Ripmeester, J. A. Communication: Single Crystal X-Ray Diffraction Observation of Hydrogen Bonding between 1-Propanol and Water in a Structure II Clathrate Hydrate. *J. Chem. Phys.* **2011**, *134*, 121104.
- (17) Subramanian, S.; Sloan, E. D. Trends in Vibrational Frequencies of Guests Trapped in Clathrate Hydrate Cages. *J. Phys. Chem. B* **2002**, *106* (17), 4348–4355.
- (18) Takeya, S.; Fujihisa, H.; Hachikubo, A.; Sakagami, H.; Gotoh, Y. Distribution of Butane in the Host Water Cage of Structure II Clathrate Hydrates. *Chem. - Eur. J.* **2014**, *20*, 17207–17213.
- (19) Tezuka, K.; Murayama, K.; Takeya, S.; Alavi, S.; Ohmura, R. Effect of Guest Size and Conformation on Crystal Structure and Stability of Structure H Clathrate Hydrates: Experimental and Molecular Dynamics Simulation Studies. *J. Phys. Chem. C* **2013**, *117*, 10473–10482.
- (20) Iino, K.; Takeya, S.; Ohmura, R. Characterization of Clathrate Hydrates Formed with CH₄ or CO₂ plus Tetrahydropyran. *Fuel* **2014**, *122*, 270–276.
- (21) Tezuka, K.; Shen, R.; Watanabe, T.; Takeya, S.; Alavi, S.; Ripmeester, J. A.; Ohmura, R. Synthesis and Characterization of a Structure H Hydrate Formed with Carbon Dioxide and 3,3-Dimethyl-2-Butanone. *Chem. Commun.* **2013**, *49* (5), 505–507.
- (22) Izumi, F.; Momma, K. Three-Dimensional Visualization in Powder Diffraction. *Solid State Phenom.* **2007**, *130*, 15–20.
- (23) Takeya, S.; Udachin, K. A.; Moudrakovski, I. L.; Susilo, R.; Ripmeester, J. A. Direct Space Methods for Powder X-Ray Diffraction for Guest–Host Materials: Applications to Cage Occupancies and Guest Distributions in Clathrate Hydrates. *J. Am. Chem. Soc.* **2010**, *132*, 524–531.
- (24) Černý, R.; Favre-Nicolin, V. Direct Space Methods of Structure Determination from Powder Diffraction: Principles, Guidelines and Perspectives. *Zeitschrift für Krist.* **2007**, *222*, 105–113.
- (25) Favre-Nicolin, V.; Černý, R. FOX, ‘free Objects for Crystallography’: A Modular Approach to Ab Initio Structure Determination from Powder Diffraction. *J. Appl. Crystallogr.* **2002**, *35*, 734–743.
- (26) Frisch, M.; Trucks, G. W.; Schlegel, H. B.; Scuseria, G. E.; Robb, M. A.; Cheeseman, J. R.; Scalmani, G.; Barone, V.; Mennucci, B.; Petersson, G. A.; et al. *Gaussian 09*, Revision C.02; Gaussian Inc.: Wallingford, CT, 2009.
- (27) Smith, W.; Forester, T. R.; Todorov, I. T. *DL_POLY2*; STFC Daresbury Laboratory: Daresbury, Washington Cheshire, U.K., 2009.
- (28) Mak, T. C. W.; McMullan, R. K. Polyhedral Clathrate Hydrates. X. Structure of the Double Hydrate of Tetrahydrofuran and Hydrogen Sulfide. *J. Chem. Phys.* **1965**, *42* (8), 2732.
- (29) Takeuchi, F.; Hiratsuka, M.; Ohmura, R.; Alavi, S.; Sum, A. K.; Yasuoka, K. Water Proton Configurations in Structures I, II, and H Clathrate Hydrate Unit Cells. *J. Chem. Phys.* **2013**, *138* (12), 124504.
- (30) Cornell, W. D.; Cieplak, P.; Bayly, C. I.; Gould, I. R.; Merz, K. M.; Ferguson, D. M.; Spellmeyer, D. C.; Fox, T.; Caldwell, J. W.; Kollman, P. A. A Second Generation Force Field for the Simulation of

Proteins, Nucleic Acids, and Organic Molecules. *J. Am. Chem. Soc.* **1995**, *117*, 5179–5197.

(31) Abascal, J. L. F.; Sanz, E.; García Fernández, R.; Vega, C. A Potential Model for the Study of Ices and Amorphous Water: TIP4P/Ice. *J. Chem. Phys.* **2005**, *122*, 234511.

(32) Harris, J. G.; Yung, K. H. Carbon Dioxide's Liquid-Vapor Coexistence Curve And Critical Properties as Predicted by a Simple Molecular Model. *J. Phys. Chem.* **1995**, *99*, 12021–12024.

(33) Martin, M. G.; Siepmann, J. I. Transferable Potentials for Phase Equilibria. 1. United-Atom Description of N-Alkanes. *J. Phys. Chem. B* **1998**, *102*, 2569–2577.

(34) Ripmeester, J. A.; Ratcliffe, C. I. The Diverse Nature of Dodecahedral Cages in Clathrate Hydrates As Revealed by ^{129}Xe and ^{13}C NMR Spectroscopy: CO_2 as a Small-Cage Guest. *Energy Fuels* **1998**, *12*, 197–200.

(35) Udachin, K. A.; Enright, G. D.; Ratcliffe, C. I.; Ripmeester, J. A. Clathrate Hydrates: Some New Structural Information. *Prepr. Symp. FUEL Chem. Am. Chem. Soc.* **1997**, *42*, 467–471.

(36) Alavi, S.; Ripmeester, J. A. Effect of Small Cage Guests on Hydrogen Bonding of Tetrahydrofuran in Binary Structure II Clathrate Hydrates. *J. Chem. Phys.* **2012**, *137*, 054712.

(37) Alavi, S.; Shin, K.; Ripmeester, J. A. Molecular Dynamics Simulations of Hydrogen Bonding in Clathrate Hydrates with Ammonia and Methanol Guest Molecules. *J. Chem. Eng. Data* **2015**, *60*, 389–397.

(38) Alavi, S.; Takeya, S.; Ohmura, R.; Woo, T. K.; Ripmeester, J. A. Hydrogen-Bonding Alcohol-Water Interactions in Binary Ethanol, 1-Propanol, and 2-Propanol + Methane Structure II Clathrate Hydrates. *J. Chem. Phys.* **2010**, *133*, 074505.

(39) Ohmura, R.; Takeya, S.; Uchida, T.; Ebinuma, T. Clathrate Hydrate Formed with Methane and 2-Propanol: Confirmation of Structure II Hydrate Formation. *Ind. Eng. Chem. Res.* **2004**, *43* (16), 4964–4966.

(40) Lee, Y.; Lee, S.; Park, S.; Kim, Y.; Lee, J.-W.; Seo, Y. 2-Propanol As a Co-Guest of Structure II Hydrates in the Presence of Help Gases. *J. Phys. Chem. B* **2013**, *117*, 2449–2455.

(41) Shin, H. S.; Lee, Y.-J.; Im, J.-H.; Han, K. W.; Lee, J.-W.; Lee, Y.; Lee, J. D.; Jang, W.-Y.; Yoon, J.-H. Thermodynamic Stability, Spectroscopic Identification and Cage Occupation of Binary CO_2 Clathrate Hydrates. *Chem. Eng. Sci.* **2009**, *64*, 5125–5130.

(42) Lee, Y.-J.; Kawamura, T.; Yamamoto, Y.; Yoon, J.-H. Phase Equilibrium Studies of Tetrahydrofuran (THF) + CH_4 , THF + CO_2 , CH_4 + CO_2 , and THF + CO_2 + CH_4 Hydrates. *J. Chem. Eng. Data* **2012**, *57*, 3543–3548.

(43) Tse, J. S.; McKinnon, W. R.; Marchi, M. Thermal Expansion of Structure I Ethylene Oxide Hydrate. *J. Phys. Chem.* **1987**, *91*, 4188–4193.